NANO LETTERS

2009
Vol. 9, No. 4
1472-1475

Intrinsic Response of Graphene Vapor Sensors

Yaping Dan,[†] Ye Lu,[‡] Nicholas J. Kybert,[‡,§] Zhengtang Luo,[‡] and A. T. Charlie Johnson*[,†,‡]

Department of Electrical and Systems Engineering, Department of Physics and Astronomy, University of Pennsylvania, Philadelphia, Pennsylvania 19104, and Department of Physics, University of Warwick, Coventry, CV4 7AL, U.K.

Received November 6, 2008; Revised Manuscript Received February 2, 2009

ABSTRACT

Graphene is a two-dimensional material with extremely favorable chemical sensor properties. Conventional nanolithography typically leaves a resist residue on the graphene surface, whose impact on the sensor characteristics has not yet been determined. Here we show that the contamination layer chemically dopes the graphene, enhances carrier scattering, and acts as an absorbent layer that concentrates analyte molecules at the graphene surface, thereby enhancing the sensor response. We demonstrate a cleaning process that verifiably removes the contamination on the device structure and allows the intrinsic chemical responses of the graphene monolayer to be measured. These intrinsic responses are surprisingly small, even upon exposure to strong analytes such as ammonia vapor.

Graphene is a zero bandgap semimetal with extraordinary electronic[1−5] and mechanical properties.[6] Comprised of a single layer of carbon with every atom on its surface, graphene is a purely two-dimensional material and an ideal candidate for use as a chemical vapor sensor. It has been reported that the absorption of individual gas molecules onto the surface of a graphene sensor leads to a detectable change in its electrical resistance.[7] It is known however that typical nanolithographic processes can leave an uncontrolled residue on graphene[8] whose impact on device transport and vapor sensing properties has not been fully explored. Moreover, the intrinsic sensitivity of graphene to gaseous vapors can only be determined through the use of samples where contamination from lithographic processing has been measured and verifiably removed. Graphene vapor sensors that are known to be free of chemical contamination should then be amenable to (bio)molecular surface modification to control their chemical sensitivity, as has been done for carbon nanotubes[9] and semiconductor nanowires.[10] They should also allow quantitative modeling of their sensor characteristics.[11]

Here we report on experiments where the structural and electron transport properties of graphene monolayer field effect transistors (FET) were measured immediately after mechanical exfoliation, after contact fabrication using electron beam lithography (EBL) and thin film deposition, and after a cleaning process based on that suggested in ref 8. Raman spectroscopy is used to confirm that samples are graphene monolayers. We find that standard EBL processing left the graphene covered by a ∼1 nm thick contamination layer that has a substantial impact on the transport properties and vapor sensor responses of the device. The contamination layer was removed by a high temperature cleaning process in a reducing (H_2/Ar) atmosphere, enabling measurements of the properties of the pristine device. Compared to the as-fabricated (contaminated) device, we find that the clean device has roughly one-third the concentration of doped carriers, four-times higher carrier mobility, and much weaker electrical response upon exposure to chemical vapors, including reactive vapors such as ammonia. An electrical current annealing process has been found to provide similar reductions in chemical doping and carrier scattering.[2,12,13]

Samples were made using mechanical exfoliation to deposit graphene sheets onto an oxidized silicon substrate (300 nm oxide thickness) with prefabricated gold alignment markers. Few-layer graphene sheets were identified by optical microscopy[14] and located with respect to the alignment markers. Atomic Force Microscopy (AFM) was used to measure the graphene thickness. Au/Cr source and drain electrodes were then fabricated using EBL and thin film evaporation. Polymethylmethacrylate (PMMA) was used as the electron beam resist (Microchem Corp., C4 950); the resist was exposed with a 30 keV electron beam at a dose of 500 μC/cm^2 and then developed according to manufacturer instructions. After electrode deposition by thermal evaporation and a liftoff step, the surface topography was again

* To whom correspondence should be addressed. E-mail: cjohnson@physics.upenn.edu.
[†] Department of Electrical and Systems Engineering, University of Pennsylvania.
[‡] Department of Physics and Astronomy, University of Pennsylvania.
[§] University of Warwick.

10.1021/nl8033637 CCC: $40.75
Published on Web 03/06/2009

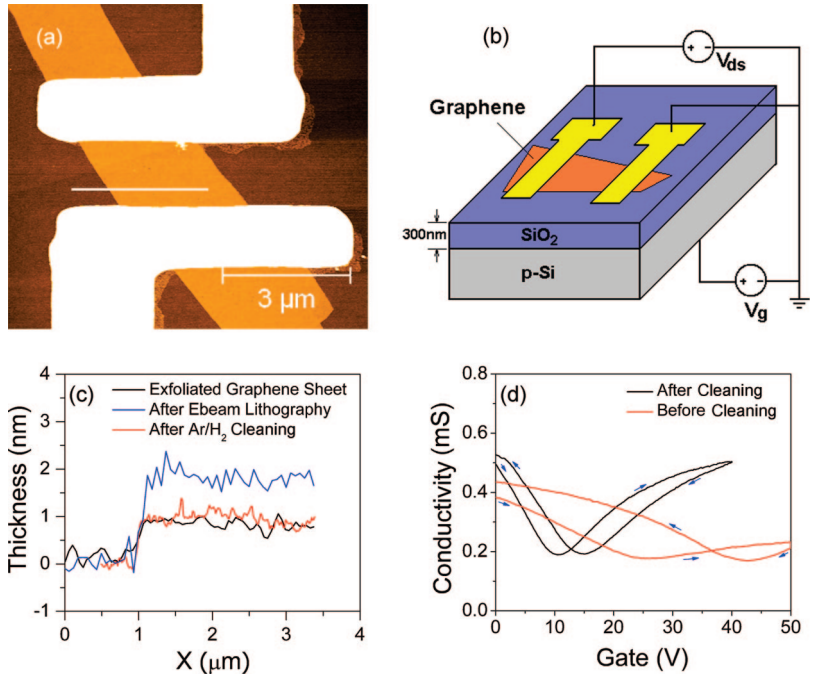

Figure 1. (a) AFM image of a graphene device. (b) Device schematic. (c) AFM line scans of the same device after exfoliation (black data; 0.8 nm thickness) after electrode fabrication by e-beam lithography (EBL) (blue data, ~2 nm thickness) and after a cleaning bake at 400 °C in Ar/H_2 (red data, 0.8 nm thickness). The Ar/H_2 cleaning process removes the residue of the EBL resist. (d) Measured electrical conductivity versus gate voltage for the device before and after cleaning (red and black data, respectively). The cleaning step leads to significantly improved electronic properties.

measured by AFM, showing evidence of contamination, presumably by residual electron beam resist (see below). We conducted current−gate voltage ($I-V_G$) measurements of the device using the p^{+2} Si substrate as the back gate, and measured changes in electrical current upon exposure to chemical vapors at varying concentration. At this point, the sample was cleaned by heating in flowing H_2/Ar (850 sccm Ar, 950 sccm H_2) at 400 °C for 1 h.[8] Finally, AFM, electron transport, and vapor response data were collected on the cleaned sample for comparison with that obtained from the contaminated device. For the vapor response measurements, gas flows containing analyte vapors of known concentration were created using a bubbler system, as described previously.[15] High purity nitrogen was used to flush the device between exposure to analyte-containing gas flows.

Figure 1a shows the AFM image of a typical graphene sample, shown schematically in Figure 1b. The as-exfoliated graphene film is 0.8 nm thick (Figure 1c, black line scan data). Raman spectroscopy measurements of identically exfoliated samples indicate that graphene films of this height are monolayers.[16,17] After EBL, the measured thickness is 1.8 nm (Figure 1c, blue data) with the thickness increase attributed to the presence of PMMA residue. From the $I-V_G$ characteristic (Figure 1d, red data) and assuming a combination of short-range and long-range carrier scattering, we find a carrier mobility of 1600 $cm^2/V{\cdot}s$.[1,3] The $I-V_G$ characteristic is hysteretic, similar to that of carbon nanotube FETs, where this phenomenon was attributed to charge injection into surface traps,[18,19] so this mechanism may be relevant to graphene devices as well. The charge neutrality point (point of minimum conductivity) occurs at $V_G \approx 30$ V, corresponding to a doped carrier density of $2.2 \times 10^{12}/cm^2$ at $V_G = 0$.

We see profound changes in the AFM data and the electrical transport measurements after the cleaning bake. AFM line scans show a sample thickness of 0.8 nm, exactly equal to that of the as-exfoliated graphene (Figure 1c, red line scan data). From the $I-V_G$ data (Figure 1d, black data), we find that the carrier mobility has increased by a factor of approximately four to 5500 $cm^2/V{\cdot}s$, and that the doped carrier density at $V_G = 0$ has been reduced by two-thirds to $7.0 \times 10^{11}/cm^2$. The hysteresis in the $I-V_G$ is much smaller than that observed before the cleaning step. We conclude that the resist residue leads to carrier doping into the graphene, increased carrier scattering, and a larger density of trap states for the carrier injection that leads to greater $I-V_G$ hysteresis. We also conclude that the cleaning step is effective and yields significantly improved structural and electronic properties of the graphene.

We find that the cleaning procedure leads to equally dramatic changes in the electrical response of the device upon exposure to chemical vapors at various concentrations (Figure 2). The analytes used were water vapor, nonanal, octanoic acid, and trimethylamine (TMA). After the EBL processing and before the cleaning bake, graphene devices show strong electrical response to these chemical vapors, even at concentrations in the part-per-billion range in the case of octanoic acid. The responses and recovery are rapid (tens of seconds) and reversible without heating or other refreshing, although irreversible "poisoning" of the sensor response is seen upon exposure to water at a concentration of 40% of a saturated vapor (Figure 2a). Changes in the $I(V_G)$ characteristics are observed that are consistent with the model that vapor

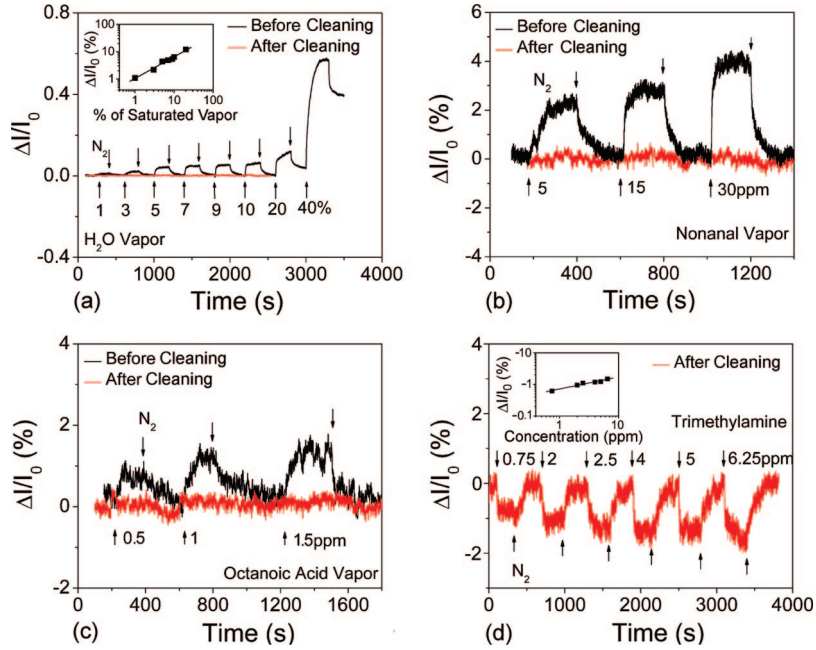

Figure 2. Measured sensor responses, before (black) and after (red) sample cleaning, to vapors of (a) water, (b) nonanal, (c) octanoic acid, and (d) trimethlyamine. The cleaning step removes resist residue from the lithography step and enables the measurement of the intrinsic responses of the graphene device. Insets: Sensor responses to water vapor and TMA show a power law dependence with exponents of 0.4 and 0.8, respectively.

molecules are bound near the sample, thereby changing the electrostatic environment for the charge carriers. For example, upon exposure to 40 ppm of dinitrotoluene (DNT), the $I(V_G)$ characteristic shifts by +1 V, indicative of chemical gating of $\sim 7 \times 10^{10}/\text{cm}^2$, and there is a mobility decrease of roughly 3% (data not shown). All sensor responses decrease sharply when the sample is cleaned and are thus not intrinsic to graphene (see below). Still, these data demonstrate that graphene vapor sensors have a number of desirable characteristics and confirm the promise of graphene for this application.

The signs of the measured vapor responses are in agreement with a model where the resist contamination acts as an unintentional "functionalization" layer that absorbs analyte molecules very near to the surface of the p-type graphene transistor, which then provides a high-sensitivity electronic readout. Water vapor is an oxidant under typical conditions (indeed, it has been suggested that the p-type behavior of graphene under ambient may be due to the effect of adsorbed water[20]), so exposure to additional water vapor is expected to increase the hole density and the current. Octanoic acid will deprotonate in the presence of adsorbed water, increasing the hole concentration (and thus the current) in the graphene by "chemical gating".[21] Trimethylamine is a proton acceptor in the presence of water, so a current decrease is expected, consistent with our observations. At this point, it is unclear whether the nonanal response is explained within this picture or involves a different mechanism. The current response typically follows a power law dependence on concentration with the exponent in the range of 0.4−0.8 (insets in Figure 2). Similar power law behavior has also been reported for vapor sensors based on metal oxides[22,23] and conducting polymer nanowires.[24]

The electrical responses to chemical vapors are reduced by 1−2 orders of magnitude after the cleaning bake. This observation is strong evidence that the EBL resist residue acts as an absorbent layer that concentrates molecules from the vapor within the polymer, less than 1 nm from the surface of the graphene. This behavior is not surprising since polymer films are sometimes used intentionally as analyte concentrators, for example, in gravimetric vapor sensors based on surface acoustic wave devices.[25]

We found that clean graphene devices show very little electrical response upon exposure to ammonia. The $I(V_G)$ characteristic shows minimal change upon exposure to concentrations as high as 1000 ppm (Figure 3a), and the current response is only about −1% at this concentration. This observation is consistent with recent first-principles calculations that predict weak binding (∼20 meV) and small charge transfer (∼0.02 e) for ammonia on graphene.[26] Results of such ab initio calculations are very sensitive to details of the computational methods used,[27] so continued work along these lines is clearly warranted. Large sensor responses in as-fabricated devices (i.e., not given a cleaning bake) are thus likely due to the presence of absorbent resist residue or other contaminants, as well as coadsorbed water on or near the device. The data presented here suggest that the last effect is weak for clean (planar) graphene devices, although it may be larger for sparse nanotube networks on a (hydrophilic) silicon oxide surface.

The results presented here illuminate a pathway toward the application of intentionally functionalized graphene devices as nanoscale sensors of molecular analytes in the vapor and liquid phase. The two-dimensional nature of graphene typically leads to devices with lower electrical

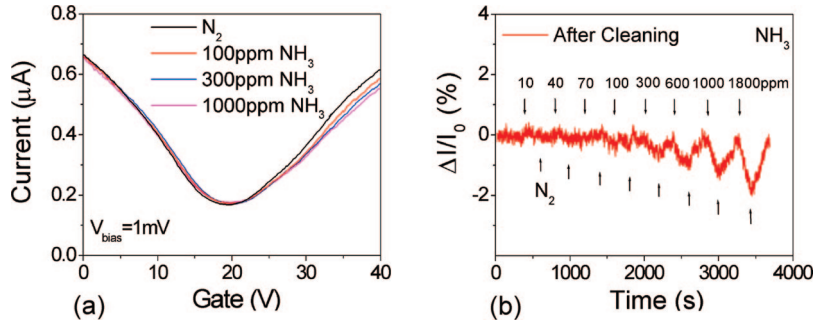

Figure 3. Sensor response to ammonia vapor. The effect on the (a) $I-V_G$ characteristic and the (b) device current are both small, even for ammonia concentrations as high as 1000 ppm.

noise, and thus lower detection limits, than those based on one-dimensional nanomaterials (e.g., carbon nanotubes and semiconductor nanowires).[7] For example, the data in Figure 2 imply that graphene sensors show rapid response and recovery, and that detection of carboxylic acids and aldehydes at ppb levels should be readily attainable. The graphene surface must be clean before strategies to control its chemical affinity via molecular functionalization may be exploited. Because of the similarity of the two nanomaterials, the cleaning process demonstrated here should enable the ready transfer to graphene of surface chemistry modifications previously applied to carbon nanotubes for targeted molecular sensing.

Acknowledgment. This work was supported by the JSTO DTRA and the Army Research Office Grant W911NF-06-1-0462. Support from the Nanotechnology Institute of the Commonwealth of Pennsylvania (Y.D.) and the REU program of the Laboratory for Research on the Structure of Matter (N.J.K.), NSF MRSEC DMR05-20020, are gratefully acknowledged.

References

(1) Morozov, S. V.; et al. Giant intrinsic carrier mobilities in graphene and its bilayer. *Phys. Rev. Lett.* **2008**, *1*.
(2) Bolotin, K. I.; et al. Ultrahigh electron mobility in suspended graphene. *Solid State Commun.* **2008**, *146*, 351–355.
(3) Chen, J. H.; Jang, C.; Xiao, S. D.; Ishigami, M.; Fuhrer, M. S. Intrinsic and extrinsic performance limits of graphene devices on SiO_2. *Nat. Nanotechnol.* **2008**, *3*, 206–209.
(4) Geim, A. K.; Novoselov, K. S. The rise of graphene. *Nat. Mater.* **2007**, *6*, 183–191.
(5) Novoselov, K. S.; et al. Two-dimensional gas of massless Dirac fermions in graphene. *Nature* **2005**, *438*, 197–200.
(6) Lee, C.; Wei, X. D.; Kysar, J. W.; Hone, J. Measurement of the elastic properties and intrinsic strength of monolayer graphene. *Science* **2008**, *321*, 385–388.
(7) Schedin, F.; et al. Detection of individual gas molecules adsorbed on graphene. *Nat. Mater.* **2007**, *6*, 652–655.
(8) Ishigami, M.; Chen, J. H.; Cullen, W. G.; Fuhrer, M. S.; Williams, E. D. Atomic structure of graphene on SiO2. *Nano Lett.* **2007**, *7*, 1643–1648.
(9) Staii, C.; Chen, M.; Gelperin, A.; Johnson, A. T. DNA-decorated carbon nanotubes for chemical sensing. *Nano Lett.* **2005**, *5*, 1774–1778.
(10) McAlpine, M. C.; et al. Peptide-nanowire hybrid materials for selective sensing of small molecules. *J. Am. Chem. Soc.* **2008**, *130*, 9583–9589.
(11) Wehling, T. O.; et al. Molecular doping of graphene. *Nano Lett.* **2008**, *8*, 173–177.
(12) Moser, J.; Barreiro, A.; Bachtold, A. Current-induced cleaning of graphene. *Appl. Phys. Lett.* **2007**, *91*.
(13) Bolotin, K. I.; Sikes, K. J.; Hone, J.; Stormer, H. L.; Kim, P. Temperature-dependent transport in suspended graphene. *Phys. Rev. Lett.* **2008**, *101*.
(14) Roddaro, S.; Pingue, P.; Piazza, V.; Pellegrini, V.; Beltram, F. The optical visibility of graphene: Interference colors of ultrathin graphite on SiO2. *Nano Lett.* **2007**, *7*, 2707–2710.
(15) Dan, Y. P.; Cao, Y. Y.; Mallouk, T. E.; Johnson, A. T.; Evoy, S. Dielectrophoretically assembled polymer nanowires for gas sensing. *Sens. Actuators, B* **2007**, *125*, 55–59.
(16) Raman spectroscopy was conducted on identically exfoliated samples, using a 514 nm wavelength laser under a 50× objective at low power (<5 mW) to avoid sample damage. Three graphene films were identified as single layer graphene by their unique Raman signatures (i.e., Stokes G peak at 1583 cm^{-1} and a single symmetric 2D band around 2700 cm^{-1}; data not shown). AFM measurements of these three films gave heights of 0.8, 1.1, and 1.0 nm.
(17) Ferrari, A. C.; et al. Raman spectrum of graphene and graphene layers. *Phys. Rev. Lett.* **2006**, *97*, 187401.
(18) Radosavljevic, M.; Freitag, M.; Thadani, K. V.; Johnson, A. T. Nonvolatile molecular memory elements based on ambipolar nanotube field effect transistors. *Nano Lett.* **2002**, *2*, 761–764.
(19) Fuhrer, M. S.; Kim, B. M.; Durkop, T.; Brintlinger, T. High-mobility nanotube transistor memory. *Nano Lett.* **2002**, *2*, 755–759.
(20) Moser, J.; Verdaguer, A.; Jimenez, D.; Barreiro, A.; Bachtold, A. The environment of graphene probed by electrostatic force microscopy. *Appl. Phys. Lett.* **2008**, *92*.
(21) Kong, J.; Dai, H. J. Full and modulated chemical gating of individual carbon nanotubes by organic amine compounds. *J. Phys. Chem. B* **2001**, *105*, 2890–2893.
(22) Rella, R.; et al. Tin Oxide-Based Gas Sensors Prepared by the Sol-Gel Process. *Sens. Actuators, B* **1997**, *44*, 462–467.
(23) Yamazoe, N.; Shimanoe, K. Theory of Power Law for Semiconductor Gas Sensors. *Sens. Actuators, B* **2008**, *128*, 566–573.
(24) Dan, Y.; Cao, Y.; Mallouk, T. E.; Evoy, S.; Johnson, A. T. C. Gas sensing properties of single conducting polymer nanowires and the effect of temperature. arXiv:0808.3199v2.
(25) Wang, F.; et al. Gate-variable optical transitions in graphene. *Science* **2008**, *320*, 206–209.
(26) Leenaerts, O.; Partoens, B.; Peeters, F. M. Adsorption of H_2O, NH_3, CO, NO_2, and NO on graphene: A first-principles study. *Phys. Rev. B* **2008**, *77*, 125416.
(27) Leenaerts, O.; Partoens, B.; Peeters, F. M. Paramagnetic adsorbates on graphene: A charge transfer analysis. *Appl. Phys. Lett.* **2008**, *92*, 243125.

NL8033637